

Transition from the macrospin to chaotic behavior by a spin-torque driven magnetization precession of a square nanoelement

D. Berkov and N. Gorn

Innovent e.V., Prüssingstrasse 27B, D-07745, Jena, Germany

(Received 20 August 2004; published 15 February 2005)

We demonstrate (using full-scale micromagnetic simulations) that the spin-injection driven steady-state precession of a thin magnetic nanoelement exhibits a complicated transition from a quasimacrospin to chaotic behavior with increasing element size. For nanoelement parameters and magnetic fields typical of those used experimentally we show that the macrospin approximation is invalid already for very small nanoelement sizes (~ 30 nm).

DOI: 10.1103/PhysRevB.71.052403

PACS number(s): 75.75.+a, 72.25.Ba, 75.70.Kw, 72.25.Pn

Magnetic excitations induced in a thin layer by a spin-polarized current injection (first predicted theoretically¹ and soon confirmed experimentally²) are at present one of the most intensively studied magnetic phenomena due to their very interesting physical nature and highly promising potential applications for, e.g., fast switching of nanoelements³ and design of nanosized dc-current driven microwave generators.⁴ Due to the complicated remagnetization processes involved it was realized very quickly⁵ that full-scale micromagnetic simulations should be carried out to support corresponding experiments, because simulations in a macrospin approximation,⁶ a necessary first step in understanding some basic physics, cannot explain many important features of the experimental observations.^{3,4}

One of the most relevant problems that could be answered by micromagnetic simulations is the determination of the critical nanoelement size for the transition from a single- to a multidomain behavior during the switching and precession process. This question was addressed in one of the first papers where full-scale micromagnetic simulations of the spin-transfer induced remagnetization were carried out.⁷ It was claimed in Ref. 7 that a nanoelement with magnetic parameters and thickness typical for real experiments remains virtually single domain for lateral size as large as 64×64 nm² up to the highest spin torque tested in the simulations (and achievable experimentally).

In this paper we present a systematic study of magnetization structures occurring during the so-called steady-state precession⁶ in square nanoelements of various sizes (to make our presentation as transparent as possible all other parameters have been fixed). We have found that the transition from a quasimacrospin precession to a multidomain state occurring by the increase of nanoelement size is very complicated; it involves several bifurcations and ends up with a fully chaotic system behavior. According to our simulations the transition to a multidomain configuration already takes place for the size ≈ 35 – 40 nm (the difference between our results and those reported in Ref. 7 is probably due to a too high exchange constant used by Li and Zhang⁸).

All parameters used in our simulations were chosen to mimic typical experimental setups described, e.g., in Refs. 3 and 4: we have simulated the steady-state precessional states for a square-shaped monolayer element with the thickness $d=2.5$ nm, saturation magnetization $M_S=950$ G, uniaxial anisotropy with the anisotropy field $H_K=500$ Oe along the $0x$ axis, exchange constant $A=2 \times 10^{-6}$ erg/cm, and Gilbert damping parameter $\lambda=0.03$ (except for the exchange value

the parameters are the same as in Ref. 7). The lateral size of a nanoelement was varied from 16×16 (where the element was single domain) to 120×120 nm² (the transition to a chaotic state completed).

Simulations were carried out using our MICROMAGUS simulation package⁹ with an additional module to include the spin injection in the form of the Slonczewski torque $\Gamma = (a_J/M_S) \cdot [\mathbf{M} \times [\mathbf{M} \times \mathbf{S}]]$ (\mathbf{S} is the spin-polarization direction of the current through a layer). All results presented here were obtained for \mathbf{S} and the external field $H_{\text{ext}}=1.75$ kOe both directed along the $0x$ axis and the spin current strength $a_J=0.4M_S$ (this is nearly twice the critical value $a_J^{\text{cr}}=0.22M_S$ for which the steady-state precession appears for $b=40$ nm). The Oersted field and thermal noise were not taken into account ($T=0$), because we intended to study a “minimal” model of the spin-torque driven magnetization dynamics (and to make our system as similar as possible to that studied in Ref. 7). The lateral mesh size was 2×2 nm². We have checked that all results were nearly independent of the discretization: doubling the number of discretization cells along each side never led to any qualitative changes of the magnetization configurations or power spectra and resulted in a shift of the spectral peak positions up to a maximum of 5%.

The coarse trend describing the system behavior with increasing element lateral size b is relatively simple. For very small sizes (up to $b \approx 20$ nm) the element behaves as a macrospin (first row in Fig. 1); the magnetization configurations for any time remain almost collinear. The three-dimensional (3D) trajectory of the average magnetization \mathbf{m}^{av} shows a well-known “out-of-plane” precession which was predicted by both single-spin⁶ and finite-element simulations.⁷ The power spectrum of m_x^{av} oscillations exhibits a very sharp peak at the precession frequency f_{prec} and much smaller peaks with rapidly decreasing amplitudes at $2f_{\text{prec}}$, $3f_{\text{prec}}$, etc., due to a slightly nonsinusoidal character of the precession.

When the element size is increased, the maximal precession angle also increases until the out-of-plane precession trajectory touches the element ($0xy$) plane (this happens for $b=32 \pm 1$ nm) and the transition to the “butterfly” trajectory occurs. The magnetization structure exhibits clear deviations from a single domain one: the maximal angle between magnetization vectors at various element points for, e.g., $b=40$ nm exceeds 45° . Although the total oscillation period increases (the limiting cycle is now much longer than for the out-of-plane precession), the spectrum peak of m_x^{av} oscillations

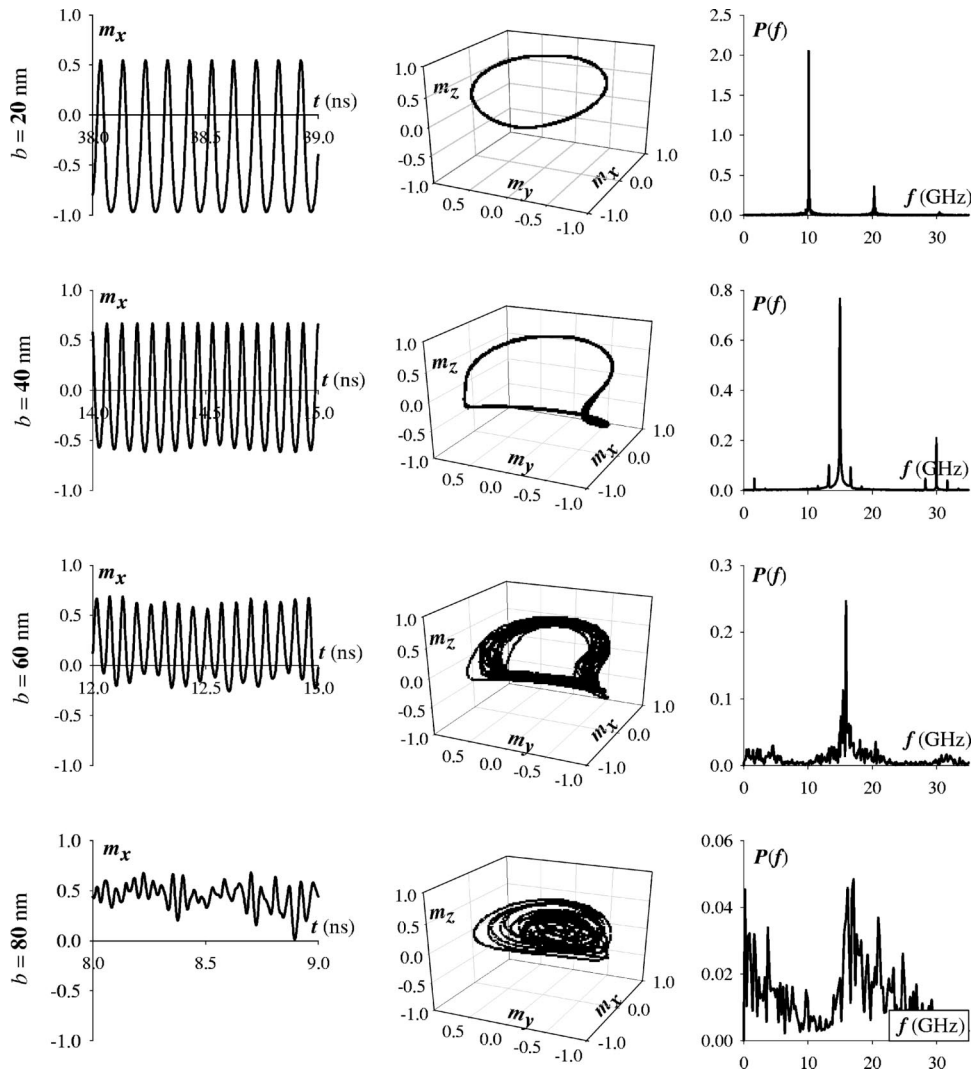


FIG. 1. Time dependencies of the x projection of the average element magnetization m_x^{av} (first column), 3D trajectories of \mathbf{m}^{av} (second column), and spectra of m_x^{av} (third column) for various element sizes as indicated on the left.

tions moves toward *higher* frequencies because one cycle includes now *two* oscillation periods for m_x^{av} (second row in Fig. 1). The weak satellites of the main spectral lines are due to a slow back-and-forth displacement of the \mathbf{m}^{av} trajectory in the region near the Oxy plane occurring in a nearly flat energy landscape in this region.

Further enlargement of the element leads to the formation of well-defined domains with clearly visible domain walls in between. This, in turn, results in the transition to a *quasiperiodic* \mathbf{m}^{av} trajectory, which now fills a bent torus (third row for $b=60$ nm in Fig. 1). The coexistence of several domains explains the broadening of the spectrum and the shift of the $m_x^{av}(t)$ dependence toward higher m_x^{av} values, due to the external field in the positive Ox direction.

For still larger element sizes the transition to the *chaotic* behavior finally occurs (see the example for $b=80$ nm in the fourth row in Fig. 1). The magnetization trajectory completely fills an area near the pole $m_x=1$, $m_y=m_z=0$. The size of the filled area decreases with increasing b due to the same aligning effect of the external field. Chaotic domain structure leads to significant changes of the average m_x^{av} value at time scales much larger than the (still visible) oscillation period. This results in a gradual transfer of the spectral power to very low frequencies.

Simulations for several intermediate system sizes reveal that the transition from the single-domain to the chaotic behavior described above contains a very interesting intermediate stage (Fig. 2). First of all we note that although the qualitative behavior of the *average* magnetization for sizes, e.g., $b=40$ and 52 nm is the same [3D \mathbf{m}^{av} trajectories of the butterfly type are observed and corresponding spectra are quite similar (the first and the last rows in Fig. 2)], magnetization patterns during the precession are very different (Fig. 3).

For $b=40$ nm the magnetization direction inside the element remains roughly the same [the maximal angle between $\mathbf{m}(\mathbf{r})$ vectors at various element points is $\sim 50^\circ$]. Pairs of semicircular quasidomains are formed near the opposite element sides during the precession (Fig. 3, upper graph) and transitions between the areas with different $\mathbf{m}(\mathbf{r})$ directions are smooth.

In contrast, the magnetization configuration for the size $b=52$ nm exhibits two well-defined domains with nearly opposite magnetization directions (Fig. 3, lower picture), and the corresponding domain wall moves up and down during the steady-state precession. The physical reason for this difference probably is that for the larger element size the total spin torques acting on different element regions are high

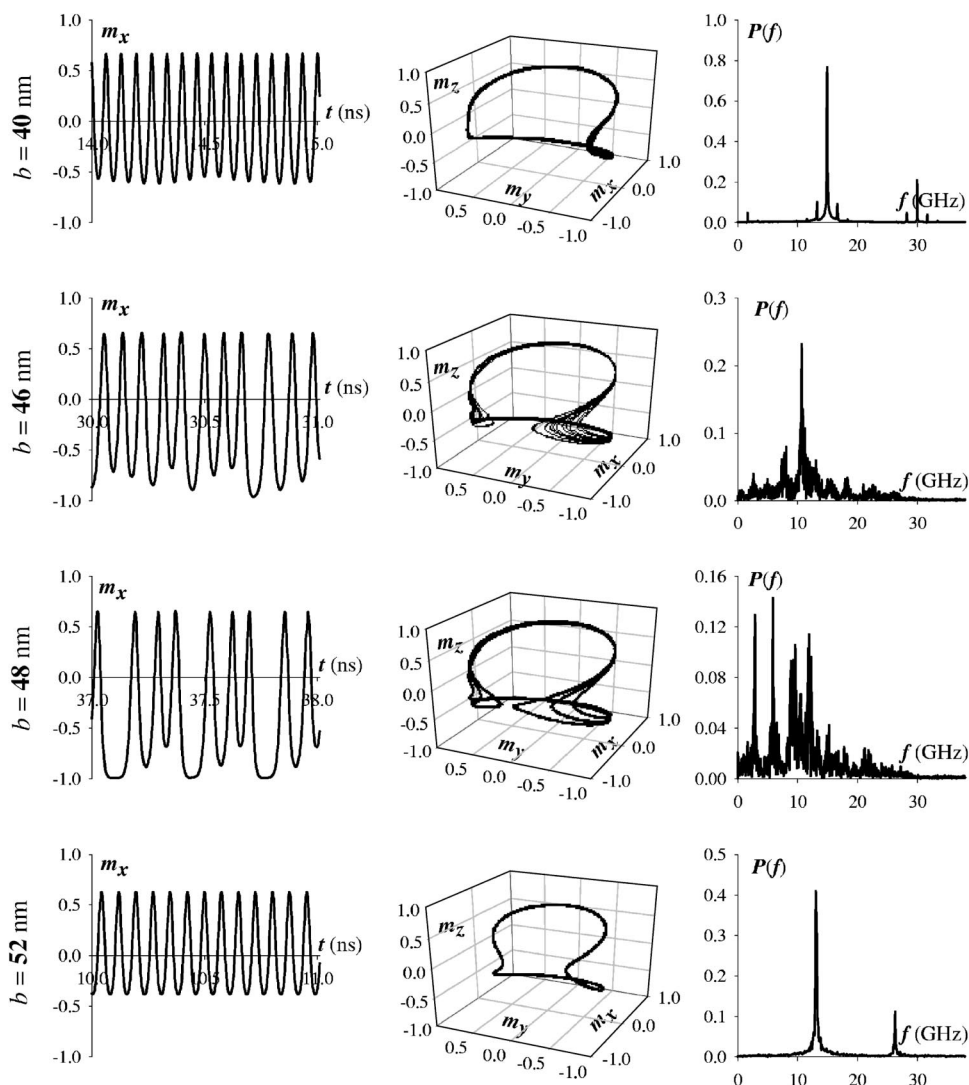


FIG. 2. The same as in Fig. 1 for element sizes from $b=40$ to 52 nm.

enough to create two relatively well-defined and nearly homogeneously magnetized domains rather than to produce a configuration with smoothly varying magnetization throughout the whole nanoelement.

The transition between the two butterfly regimes described above occurs in a very interesting way. When the size is increased above $b=40$ nm, the limiting cycle broadens into a band of trajectories whose width is maximal in the already mentioned critical region near the $0xy$ plane (see the 3D trajectory for $b=46$ nm in the second row in Fig. 2); this also results in the shift and broadening of the main spectral line. On a further (very small) size increase up to $b=48$ nm the continuous band of trajectories splits itself and all trajectories collapse into three limiting subcycles (third row in Fig. 2). A peak at a frequency much lower than that of a normal precession corresponding to the complete motion cycle over all these three subcycles appears in the spectrum, together with its harmonics. And, finally, the size increase up to $b=52$ nm let all the subcycles collapse into a single butterfly-type limiting cycle.

The detailed discussion of these results will be given elsewhere. Here we only mention that, according to our simulations, the transitions studied above are shifted, as expected,

toward higher lateral sizes when the exchange constant and/or the element thickness is increased. The smoothing of sharp corners of a square element also stabilizes to some extent the homogeneous magnetization state. However, for all studied values of the exchange constants (up to $A=4 \times 10^{-6}$ erg/cm), all thicknesses up to $d=5$ nm, and all smoothing radii (up to a circular shape) the element with the lateral size $b=120$ nm was always at least in a multidomain state. Inclusion of the Oersted field shifts all transitions toward *smaller* sizes because this field is strongly inhomogeneous.

The influence of thermal noise on these processes requires careful investigation (except for the trivial statement that this noise is expected to shift the transition sizes toward smaller dimensions), especially in view of recent important insights into the general problem of thermal fluctuations in numerical micromagnetics.¹⁰ Whether thermal noise will mask the fine features shown in Fig. 2 is not clear in advance; for example, even for a smaller element with lower exchange¹¹ some fine features of the limiting cycles in the multidomain region are still clearly visible for $T=300$.

Some brief comments concerning theoretical interpretation of our results and their relation to earlier simulations and

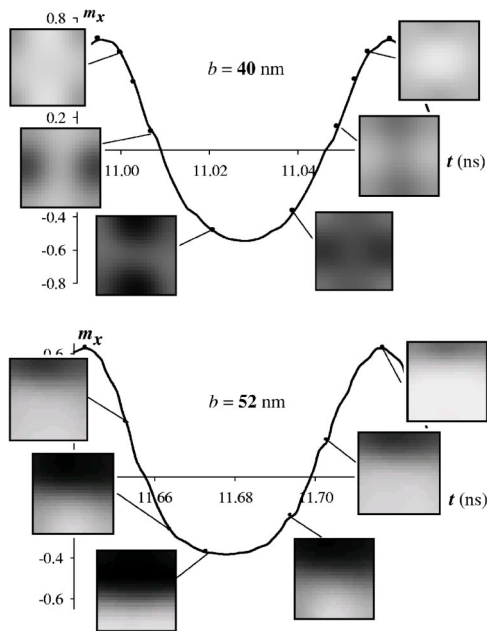


FIG. 3. Comparison of magnetization patterns during the steady-state precession for elements with the sides $b=40$ and 52 nm.

experimental observations are in order. First we note that a theoretical analysis of our data obviously requires the application of the nonlinear dynamics formalism.¹² For example, the qualitative changes of trajectories shown in Fig. 2 strongly resemble pictures of processes known as “period multiplication” bifurcations; the time-dependent trajectories for, e.g., $b=48$ nm are very similar to those known from Lorentz attractor studies;¹² and the overall behavior of the system when its size is increased obviously represents a nice example of the transition from regular to chaotic behavior when one of the system parameters (the nanoelement size in our case) is varied.¹²

However, we point out that the corresponding rigorous analysis will be extremely difficult. The reason is that our system is actually a $2N$ -dimensional one, where $N=N_x \times N_y$ is the total number of discretization cells. This means that trajectories of the *average* magnetization shown in Fig. 1 and 2 are *not* the trajectories in the system phase space which are required for the analysis with nonlinear dynamics methods, but merely the trajectories of certain low-dimensional (3D) functionals defined on this phase space. The complete analy-

sis of the system behavior in terms of Lyapunov exponents would require the (very precise) determination of the eigenvalues of corresponding $2N \times 2N$ matrices, which is a tedious computational task, leaving apart the rather nontrivial interpretation problem of the resulting sets of $2N$ eigenvalues. For these reasons we believe that such studies should be carried out only if one expects from them new deep insights into the physics of the process beyond those that can be obtained by studying standard physical characteristics as discussed above.

Our results can also be compared with simulations from Refs. 13–15, where a transition from the quasimonodomain to a multidomain and further to a chaotic state with increasing *current strength* was “observed” for elliptical 100×50 nm² Permalloy¹³ and 130×70 nm² Co (Ref. 15) single-layer elements. In Refs. 13 and 15 similar kinds of magnetization oscillation spectra for a steady-state precession were obtained. The spin current strength $a_J=0.4M_S$ used in our simulations corresponds to the current values where the chaotic magnetization behavior in Refs. 13 and 15 was observed. Hence, taking into account the relatively large element sizes used in Refs. 13 and 15, we conclude that for this particular region of sizes and currents our results are in qualitative agreement with Refs. 13 and 15.

Results like those shown here may be in principle compared *directly* with high-quality experimental measurements of the spin-transfer induced microwave oscillation spectra available now.⁴ However, our simulations demonstrate that for the nanoelement sizes commonly used in such experiments, the nature of the precessional state (which is necessary to ensure the very existence of nondecaying, microwave oscillations) is very sensitive to the element size. Furthermore (corresponding results will be reported elsewhere) the shape of the element and its polycrystalline structure (for materials with significant magnetocrystalline anisotropy) also play an important role. Apart from the evident conclusion that simulations of a spin-torque induced precession of nanoelements with experimentally interesting sizes in a macrospin approximation are not very helpful, our results show that a *precise* determination of all above mentioned physical parameters of the experimentally studied system is required to enable a meaningful comparison with micromagnetic simulations. The latter step is, in turn, necessary for a real understanding of physical processes underlying the magnetization dynamics in the presence of a spin-polarized current.

¹J. C. Slonczewski, J. Magn. Magn. Mater. **159**, L1 (1996); L. Berger, Phys. Rev. B **54**, 9353 (1996).

²J. Z. Sun, J. Magn. Magn. Mater. **202**, 157 (1999); M. Tsoi *et al.*, Phys. Rev. Lett. **80**, 4281 (1998).

³J. A. Katine *et al.*, Phys. Rev. Lett. **84**, 3149 (2000); J. Grollier *et al.*, Appl. Phys. Lett. **83**, 509 (2003); F. B. Mancoff *et al.*, *ibid.* **83**, 1596 (2003).

⁴S. I. Kiselev *et al.*, Nature (London) **425**, 380 (2003); W. H. Rippard *et al.*, Phys. Rev. Lett. **92**, 027201 (2004).

⁵J. Miltat *et al.*, J. Appl. Phys. **89**, 6982 (2001).

⁶J. Z. Sun, Phys. Rev. B **62**, 570 (2000).

⁷Z. Li and S. Zhang, Phys. Rev. B **68**, 024404 (2003).

⁸Z. Li (private communication).

⁹D. V. Berkov and N. L. Gorn, <http://www.micromagus.de>

¹⁰G. Grinstein and R. H. Koch, Phys. Rev. Lett. **90**, 207201 (2003).

¹¹D. V. Berkov and N. L. Gorn, cond-mat/0409098, J. Magn. Magn. Mater. (to be published).

¹²V. S. Anishchenko *et al.*, *Non-Linear Dynamics of Chaotic and Stochastic Systems* (Springer, Berlin, 2002).

¹³X. Zhu *et al.*, J. Appl. Phys. **95**, 6630 (2004).

¹⁴J.-G. Zhu and X. Zhu, IEEE Trans. Magn. **40**, 182 (2004).

¹⁵K. J. Lee *et al.*, Nat. Mater. **3**, 877 (2004).